The ETS-5 transcription factor regulates activity states in *Caenorhabditis elegans* by controlling satiety

Vaida Juozaityte[a,b], David Pladevall-Morera[a,b], Agnieszka Podolska[a], Steffen Nørgaard[a,b], Brent Neumann[c], and Roger Pocock[a,b,1]

[a]Development and Stem Cells Program, Monash Biomedicine Discovery Institute and Department of Anatomy and Developmental Biology, Monash University, Melbourne, VIC 3800, Australia; [b]Biotech Research and Innovation Centre, University of Copenhagen, DK-2200 Copenhagen, Denmark; and [c]Neuroscience Program, Monash Biomedicine Discovery Institute and Department of Anatomy and Developmental Biology, Monash University, Melbourne, VIC 3800, Australia

Edited by Gary Ruvkun, Massachusetts General Hospital, Boston, MA, and approved January 10, 2017 (received for review June 30, 2016)

Animal behavior is shaped through interplay among genes, the environment, and previous experience. As in mammals, satiety signals induce quiescence in *Caenorhabditis elegans*. Here we report that the *C. elegans* transcription factor ETS-5, an ortholog of mammalian FEV/Pet1, controls satiety-induced quiescence. Nutritional status has a major influence on *C. elegans* behavior. When foraging, food availability controls behavioral state switching between active (roaming) and sedentary (dwelling) states; however, when provided with high-quality food, *C. elegans* become sated and enter quiescence. We show that ETS-5 acts to promote roaming and inhibit quiescence by setting the internal "satiety quotient" through fat regulation. Acting from the ASG and BAG sensory neurons, we show that ETS-5 functions in a complex network with serotonergic and neuropeptide signaling pathways to control food-regulated behavioral state switching. Taken together, our results identify a neuronal mechanism for controlling intestinal fat stores and organismal behavioral states in *C. elegans*, and establish a paradigm for the elucidation of obesity-relevant mechanisms.

ETS transcription factor | neuronal signaling | satiety | fat levels | quiescence

Animal behavior is strongly influenced by the availability of food. In invertebrates and vertebrates, appetite, locomotor activity, and sleep rhythms are all driven by nutritional state (1–7). When malnourished, animals seek out a new food source by actively exploring their environment (roaming), whereas animals that are well fed tend to explore less (dwelling) and when fully sated enter a quiescent or sleep-like state (1–3, 8, 9). Transitions between these behavioral states can be regulated by sensory perception of external stimuli and through gut signals or other internal cues that are generated according to food quality (3, 4, 6).

Initial evidence for neuronal regulation of feeding behavior was shown in mammals using hypothalamic lesions (10). Sectioning of specific regions within the rat hypothalamus evoked opposing behaviors. Removal of one section caused overeating and obesity, whereas removal of an adjacent section resulted in starvation owing to reduced eating (10). Subsequent studies showed that the pro-opiomelanocortin–expressing neurons in the hypothalamus function to suppress feeding, whereas a hypothalamic region that contains neuropeptide Y/agouti-related protein–expressing neurons promotes feeding (11). These adjacent brain regions integrate signals received from the gut that report satiety (12). The nutritive content of food itself also serves as a potent regulator of behavior. In mammals, a diet loaded with fats and sugars stimulates overfeeding and leads to obesity (13). In addition, rats can learn to select a source of food based exclusively on its nutritional value in the absence of external cues (14).

In *Caenorhabditis elegans*, as in mammals, nutritive value is a behavioral stimulus (1, 4). Nematodes exhibit different behaviors when cultured on low-quality food compared to high-quality food, with high-quality food defined as a superior supporter of worm growth (1, 4). Sensory perception of food in the environment can promote roaming, whereas internal perception of food abundance in the intestine promotes dwelling (3). As such, animals that are unable to sense their environment, and thus cannot sense the presence of food, exhibit reduced time spent roaming (9).

When fed on the standard laboratory *Escherichia coli* strain (OP50, a low-quality food), *C. elegans* spontaneously transition between dwelling and roaming, and are quiescent <5% of the time (1). This suggests that nematodes are not fully sated in laboratory conditions and hence increase their roaming behavior to search for a more optimal environment. In support of this idea, when grown on high-quality bacteria, *C. elegans* are >90% quiescent due to satiety (1). At a behavioral level, this quiescent state is reminiscent of postprandial somnolence in mammals. Postprandial somnolence is thought to reflect an increase in the tone of the parasympathetic nervous system relative to the sympathetic nervous system, as well as altered activity of arousal circuits as a result of increased blood glucose levels, although the pathways mediating these effects are poorly understood (15). In *C. elegans*, neuronal signaling pathways using serotonin (5-HT), pigment-dispersing factor (PDF) neuropeptides, TGF-β, and the cGMP-dependent protein kinase EGL-4 regulate roaming, dwelling, and quiescent behaviors (1–3, 9). These modulators of food-regulated behavior function in dedicated, mostly nonoverlapping neuronal circuits that detect environmental cues, along with evaluating internal metabolic status (2); however, the transcriptional control of food-regulated behaviors has not yet been defined.

The ETS (E twenty-six) family is one of the largest transcription factor (TF) families in metazoa. In humans, there are 29 family members, whereas in *C. elegans*, there are 10, with representative members of all of the major classes (16–18). ETS TFs use their conserved 85-aa winged helix-turn-helix ETS

Significance

Animals constantly monitor their internal energy levels and modify their eating and foraging behavior as required. Our work defines a role for the ETS-5 transcription factor in the control of body fat levels and thereby the activity of animals. We have defined the responses controlled by ETS-5 at the genetic, cellular, and organismal levels and identified how ETS-5 interacts with known pathways that regulate food-regulated behavioral states. These findings provide insight into how fat levels are regulated and how satiety controls organismal activity.

Author contributions: V.J., D.P.-M., A.P., B.N., and R.P. designed research; V.J., D.P.-M., A.P., S.N., B.N., and R.P. performed research; V.J., D.P.-M., A.P., B.N., and R.P. contributed new reagents/analytic tools; V.J., D.P.-M., A.P., B.N., and R.P. analyzed data; and V.J., D.P.-M., A.P., B.N., and R.P. wrote the paper.

The authors declare no conflict of interest.

This article is a PNAS Direct Submission.

Freely available online through the PNAS open access option.

[1]To whom correspondence should be addressed. Email: roger.pocock@monash.edu.

This article contains supporting information online at www.pnas.org/lookup/suppl/doi:10.1073/pnas.1610673114/-/DCSupplemental.

domain to interact with regulatory elements of target genes harboring purine-rich DNA sequences (19–21). Members of the ETS TF family are functionally diverse; in *C. elegans*, for example, AST-1/ETV1 regulates axon guidance and dopaminergic neuron differentiation (22, 23), LIN-1/ELK3 regulates vulval development downstream of MAP kinase signaling (24), and ETS-4/SPDEF controls lifespan (25). We and others have previously shown that ETS-5/FEV controls the carbon dioxide-sensing function of the BAG neurons (26, 27). In vertebrates, the homologs of ETS-5, FEV(human)/Pet1(mouse), also play prominent roles in brain development and function, including the control of circadian rhythms, as well as anxiety-like and aggressive behaviors (28–30).

We sought to identify additional neuronal functions of ETS-5 by screening for behavioral phenotypes in *ets-5* loss-of-function mutant animals. Using this approach, we discovered that *ets-5* is required for food-regulated behavioral state switching. When cultured on low-quality food, *ets-5* mutant animals exhibit reduced roaming and an increase in quiescent behavior, suggesting that they are more sated, or perceive that they are sated, even on low-quality food. This behavioral change was abrogated when *ets-5* mutant animals were malnourished, suggesting that internally generated metabolic signals regulate the changes in behavior. Indeed, we found that *ets-5* mutants stored excess fat, and that a reduction in fatty acid biosynthesis suppressed the exploratory defects of these animals. Finally, we show that *ets-5* acts in the ASG and BAG sensory neurons to control exploratory behavior, most likely through the action of multiple neuropeptides.

Taken together, our findings identify a function of the conserved ETS-5 TF in food-regulated behavioral state switching that is controlled by internal metabolic signals of satiety. In mammals, ETS TFs are associated with obesity regulation and behavioral states (31, 32) pointing to a potentially conserved regulatory function.

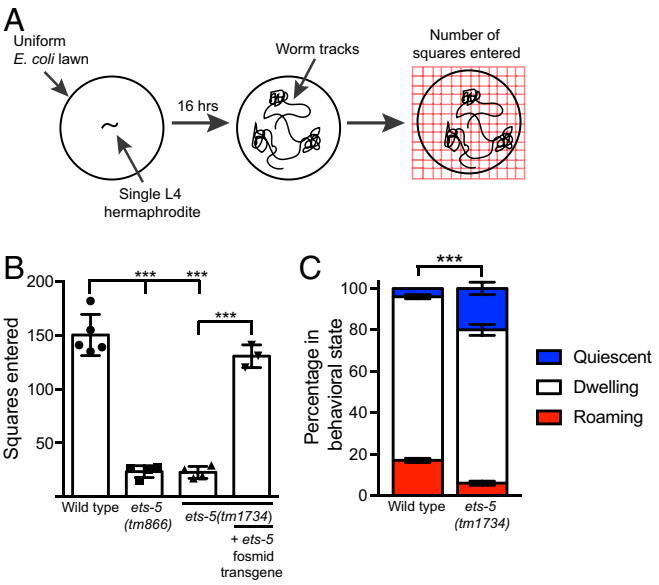

Fig. 1. ETS-5 controls exploratory behavior. (*A*) Schematic of the assay used to evaluate exploration behavior across a bacterial lawn. The grid has 250 squares. The number of squares entered can vary from day to day; thus, all genetic manipulations are compared with controls tested in parallel. (*B*) Two independent mutant alleles of *ets-5* (*tm866* and *tm1734*) are defective in exploring a bacterial lawn. The exploration defect of *ets-5(tm1734)* mutant animals can be rescued through transgenic expression of an *ets-5::GFP*–expressing fosmid. At least three independent replicates are shown ($n > 20$ per replicate). ***$P < 0.001$, ANOVA with Tukey's multiple comparisons test. (*C*) Proportions of WT and *ets-5(tm1734)* mutant animals in the roaming, dwelling, and quiescent states. $n > 100$. ***$P < 0.001$, *t* test.

Results

The ETS-5 Transcription Factor Is Required for Exploratory Behavior in *C. elegans*. When cultured on a standard laboratory bacterial lawn (OP50 *E. coli*), we noticed that *ets-5* null mutant animals do not explore their environment to the same extent as wild-type (WT) animals. To quantify this defect, we used a well-established exploratory behavior paradigm (2). In this assay, single larval stage 4 (L4) animals were placed in the center of a nematode growth medium (NGM) agar plate that was completely coated with a lawn of OP50 *E. coli* bacteria, and the tracks the animals made over a 16-h period were recorded (Fig. 1*A* and Fig. S1*A*). Compared with WT animals, the *ets-5* null mutant animals exhibited an approximate 10-fold reduction in exploratory capacity (Fig. 1*B*). Both of the *ets-5*–predicted null alleles that we analyzed exhibited similar defects in exploratory behavior, and we rescued the *ets-5(tm1734)* mutant phenotype using an *ets-5::gfp* fosmid transgene (Fig. 1*B*).

The significantly reduced exploration exhibited by the *ets-5* mutant animals could be caused by general defects in neuronal function and/or locomotion. However, we found that the loss of *ets-5* did not cause a detectable change in locomotor speed or in the ability to sense and respond to gustatory and olfactory cues (Fig. S1 *B–F*), indicating that the exploratory defect observed in the *ets-5* mutant animals was not caused by general defects in locomotion or in the ability to sense external cues in the environment.

To more precisely define the effect of *ets-5* loss on exploratory capacity, we studied the behavioral state of individual worms. We detected three behavioral states in this analysis: roaming, dwelling and quiescence, as described previously (1). Roaming animals moved forward rapidly, turning infrequently; dwelling animals either turned frequently in a localized area or remained stationary while pumping the pharynx; and quiescent animals did not move or pump the pharynx during the 10-s analysis period (1, 2). We found that the proportions of WT animals in the roaming (21%), dwelling (75%), and quiescent (4%) states were similar to those reported previously (1) (Fig. 1*C*). In *ets-5* mutant animals, the proportion of dwelling animals was unchanged (73%), whereas that of roaming animals was reduced (8%) and that of quiescent animals was increased (19%) (Fig. 1*C*). Taken together, these data indicate that *ets-5* is required to control the behavioral state of *C. elegans*, in which *ets-5* loss causes reduced activity.

***ets-5* Acts in the ASG and BAG Sensory Neurons to Control Exploratory Behavior.** To elucidate the focus of action for ETS-5 in the regulation of exploratory behavior, we analyzed the full 4-kb upstream intergenic region of *ets-5* and found that it drives the expression of a fluorescent reporter in two pairs of neurons (Fig. 2*A*). Based on position, morphology, and colocalization with neuron-specific reporters, we identified these neurons as ASGL/R and BAGL/R (Fig. 2*A* and Fig. S2*A*). We found that the *ets-5(tm1734)* exploration defect was rescued in transgenic animals expressing *ets-5* cDNA under control of the *ets-5* promoter (Fig. 2*B*), suggesting that the expression of *ets-5* in these neurons controls exploratory behavior. To reinforce these data, we performed neuron-specific RNA-mediated interference (RNAi) of *ets-5* in the ASG and BAG neurons, and found that exploratory behavior was diminished (Fig. 2*C*). These data demonstrate that *ets-5* acts in the ASG and/or BAG neurons to regulate exploratory behavior in *C. elegans*.

To confirm the importance of the ASG and BAG neurons in exploration, we performed genetic and laser ablation experiments (Fig. 2 *D* and *E* and Fig. S2*B*). We first used a laser microbeam to kill the ASG and BAG neurons and then assayed the exploratory capacity of ablated animals. We found that ablation of either the ASG or BAG neurons reduced exploration (Fig. S2*B*). For technical reasons, we were unable to reliably laser-kill the ASG and BAG neurons in the same animal, and thus we

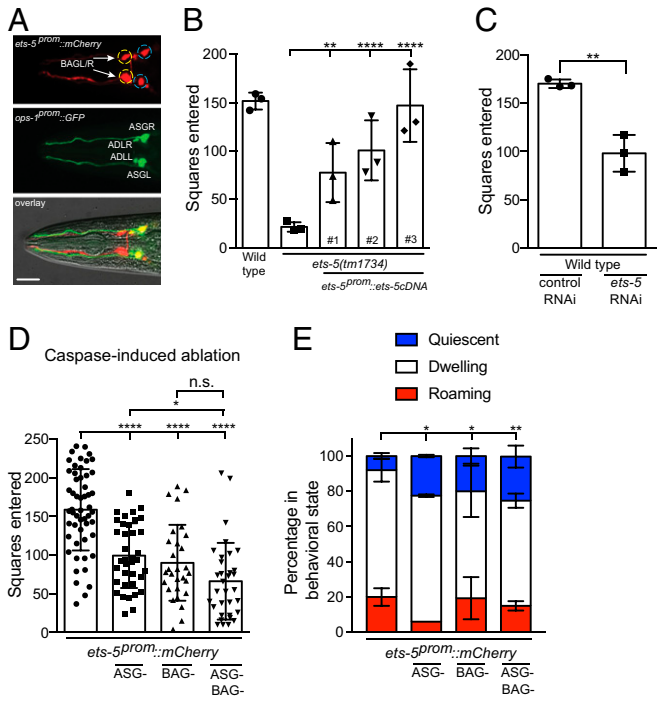

Fig. 2. *ets-5* acts in the ASG and BAG neurons to control exploratory behavior. (*A*) The *ets-5* promoter drives expression of mCherry protein in the BAG neurons (Fig. S2), as reported previously (26, 27), and ASG neurons. (*Top*) *ets-5^{prom}mCherry* reporter. (*Middle*) *ops-1^{prom}::GFP* reporter, expressed in the ASG and ADL neurons. (*Bottom*) Overlay with DIC. Anterior is to the left. (Scale bar: 20 μm.) (*B*) Expression of *ets-5* cDNA controlled by the 4-kb *ets-5* promoter (BAG- and ASG-expressed) rescues the exploratory defect of *ets-5(tm1734)* mutant animals. # refers to independent transgenic lines. Three independent replicates are shown (n >20 per replicate). $^{**}P < 0.001$, $^{****}P < 0.0001$, ANOVA with Tukey's multiple comparisons test. (*C*) BAG- and ASG-specific RNAi, using the *ets-5* promoter to drive *ets-5* snapback RNA, reduced exploratory behavior of WT animals. The *ets-5^{prom}::mCherry* cotransformation marker was injected into WT animals for the control. Three independent replicates are shown (n >10 per replicate). $^{**}P < 0.002$, Mann–Whitney U test. (*D*) Caspase-induced ablation of either the ASG or BAG neurons reduced exploratory behavior of *ets-5^{prom}::mCherry*–expressing animals. Ablating both the ASG and BAG neurons caused a further reduction in exploratory behavior. n >29. $^{****}P < 0.0001$, ASG or BAG compared with control; $^{*}P < 0.01$ comparing ASG and ASG/BAG; n.s., not significantly different between BAG ablation and ASG-BAG ablation, ANOVA with Tukey's multiple comparisons test. (*E*) Caspase-induced ablation of either the ASG or BAG neurons increased the fraction of animals in the quiescent state compared with controls. In contrast, only ASG ablation caused a reduction in roaming. n >29. $^{*}P < 0.05$, $^{**}P < 0.01$, ANOVA with Tukey's multiple comparisons test.

turned to the split caspase genetic ablation system (33). As in the laser ablation experiments, caspase-induced genetic ablation of either the ASG or BAG neurons reduced exploration (Fig. 2*D*). We also found that ablation of both the ASGs and BAGs resulted in a further reduction of exploratory capacity, resembling *ets-5* mutant animals (Fig. 2*D*). In concurrence with this finding, behavioral state analysis of ASG ablation, BAG ablation, and ASG and BAG ablation showed an increase in quiescence compared with controls (Fig. 2*E*). These data confirm the roles of the ASG and BAG neurons in the regulation of exploratory behavioral states in *C. elegans*.

ETS-5 Mutant Defects in Oxygen- and Carbon Dioxide-Sensing Function Do Not Affect Exploratory Behavior. Previous studies have shown that ETS-5 specifies the oxygen- and carbon dioxide-sensing neuron fate of the BAG neurons (26, 27). ETS-5 is required for BAG expression of the CO_2-sensing receptor-type guanylate cyclase GCY-9 and the O_2-sensing soluble guanylate cyclases GCY-31 and GCY-33. As such, *ets-5* mutant animals are unable to coordinate behavioral responses to CO_2 exposure or to downsteps in O_2 levels (Fig. S1 *B* and *C*) (26, 27). We tested whether these deficits in O_2- and CO_2-sensing function in *ets-5* mutant animals may be responsible for their reduced exploratory capacity. We analyzed the *gcy-9(n4470)* mutant (loss of BAG-regulated CO_2 sensing), the *gcy-31(ok296); gcy-33(ok232)* double mutant (loss of BAG-regulated O_2 sensing) and the *gcy-9(n4470) gcy-31(ok296); gcy-33(ok232)* triple mutant (loss of BAG-regulated O_2 and CO_2 sensing) (Fig. S2*C*). We found that none of these mutant backgrounds caused a significant change in exploratory behavior, indicating that defective O_2 and CO_2 sensing in *ets-5* mutant animals does not cause the exploration defects (Fig. S2*C*).

***ets-5* Functions in a Complex Genetic Network with 5-HT, PDF, and cGMP Signaling to Control Behavioral State Switching.** Previous work has shown that the dwelling, or resting, state is promoted by 5-HT signaling, and that the roaming, or active, state is promoted by PDF signaling (2). In addition, EGL-4 cGMP-dependent protein kinase signaling inhibits roaming and promotes quiescence (1, 9). To better understand the genetic hierarchy between these pathways and the behavioral state regulator ETS-5, we performed double-mutant genetic analysis. The exploration assay shown in Fig. 1*B* provided some epistatic information (Fig. S3); however, the resolution was low, and it was unable to gauge quiescence. Therefore, we also directly studied the behavioral state of single worms as shown in Fig. 1*C*.

To assay behavioral states and exploration, we first crossed *ets-5(tm1734)* mutants with animals mutant for *mod-1(ok103)*, which encodes a 5-HT-gated chloride channel previously shown to suppress roaming (Fig. 3*A* and Fig. S3*A*) (2). In concurrence with this work, we found that the loss of *mod-1* increased exploration; however, in *mod-1*; *ets-5* double mutant animals, we observed the *ets-5* mutant phenotype (Fig. S3*A*). This finding suggests that *ets-5* acts genetically downstream of 5-HT signaling to control exploration behavior. However, when we studied the behavioral states of these animals directly, we found that loss of MOD-1–dependent 5-HT signaling suppressed the increased quiescence, but not the reduced roaming, of *ets-5* mutant animals (Fig. 3*A*). This finding suggests that defective neuronal signaling in *mod-1* mutant animals switches the behavioral state of *ets-5* mutants from quiescent to dwelling.

We next performed a similar analysis with the PDF-1 pathway. Loss of PDF signaling using the PDF-1/2 receptor mutant *pdfr-1(ok3425)* resulted in exploratory behavior similar to that exhibited by *ets-5* mutant animals (Fig. S3*B*). The *ets-5; pdfr-1* double mutant explored to a similar degree as each single mutant, thus preventing any further resolution. Using behavioral state analysis, we found that the *ets-5; pdfr-1* double mutant exhibited similar quiescence and lack of roaming as the *pdfr-1* single mutant (Fig. 3*B*). This finding suggests that PDFR-1 acts downstream of *ets-5* to control behavioral state. Finally, we confirmed a previous report that cGMP signaling inhibits roaming (9), showing that *egl-4(n479)* loss-of-function animals explored more than WT animals (Fig. S3*C*). When the *egl-4(n479)* and *ets-5(tm1734)* mutations were combined, WT exploration was restored (Fig. S3*C*), and in the behavioral state assay, *egl-4* was epistatic to *ets-5* (Fig. 3*C*). This finding suggests that EGL-4 acts downstream of ETS-5 in the regulation of exploration. Taken together, these data present a complex network comprising a TF (ETS-5) and conserved neuronal signaling pathways (5-HT, PDF, and cGMP) that control behavioral states in *C. elegans* (Fig. 3*D*). It predicts that exquisite control of neuronal signaling by these factors can modulate the behavioral state of animals to optimize their survival potential in ephemeral environments.

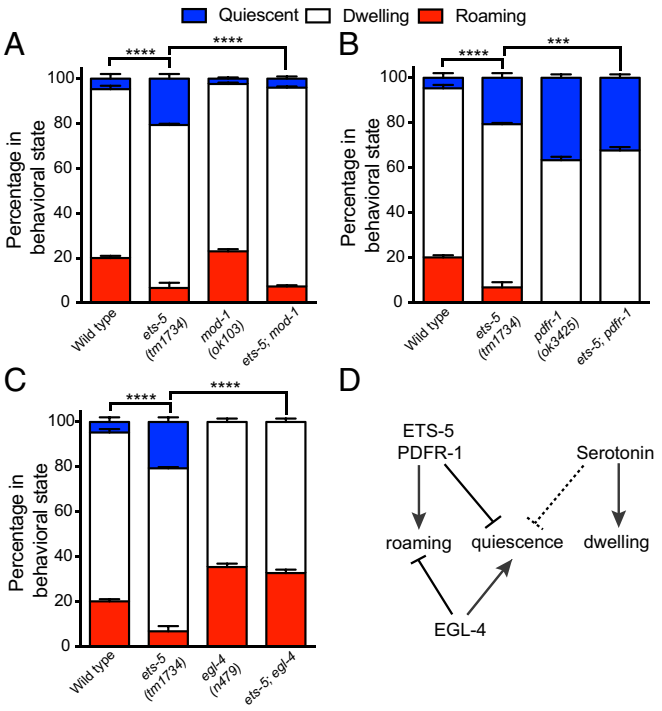

Fig. 3. Genetic epistasis analysis between *ets-5* and known signaling pathways that control exploratory behavior. (*A*) 5-HT signaling promotes dwelling and has a subtle role in suppressing quiescence. *ets-5* is epistatic to 5-HT signaling in the control of roaming; however, in *ets-5; mod-1* double-mutant animals, the enhanced quiescence of *ets-5* mutants is suppressed. $n > 80$. $^{****}P < 0.0001$, ANOVA with Tukey's multiple comparisons test. (*B*) PDF signaling promotes roaming and inhibits quiescence. *ets-5; pdfr-1* double-mutant animals exhibit similar quiescence levels as each single mutant. $n > 80$. $^{***}P < 0.001$, $^{****}P < 0.0001$, ANOVA with Tukey's multiple comparisons test. (*C*) EGL-4 cGMP-dependent protein kinase signaling strongly inhibits roaming behavior and promotes quiescence. *ets-5; egl-4* double-mutant animals exhibit the *egl-4* mutant phenotype. $n > 80$. $^{****}P < 0.0001$, ANOVA with Tukey's multiple comparisons test. (*D*) The molecular pathways that control roaming, dwelling, and quiescence. The dotted line represents proposed weak regulation.

Malnutrition Suppresses Exploration Defects Caused by Loss of ETS-5. It was previously shown that satiety, engendered by high-quality food, induces quiescence (1). We hypothesized that the sixfold increase in quiescence in *ets-5* mutant animals could be a result of enhanced satiety or a perception of satiety. Therefore, we tested whether reducing satiety through chemically induced or genetically induced malnutrition could modify the *ets-5* mutant phenotype (Fig. 4 *A* and *B*). First, we treated OP50 *E. coli* bacteria with the antibiotic aztreonam, which prevents bacterial division and produces filamentous bacteria that are inedible to worms (3, 34). When *ets-5* mutant animals were placed on exploration plates containing this inedible food, their exploratory ability was restored to WT levels (Fig. 4*A*). This effect of malnutrition occurred rapidly; a time-course experiment showed that *ets-5* mutant animals explored similarly as WT animals as early as 1 h after being transferred to aztreonam-treated bacterial plates (Fig. S4).

The suppression of the *ets-5* mutant exploratory defects by aztreonam-treated bacteria could be due to a sensory response to poor (inedible) food or to an internal starvation/metabolic response. To distinguish between these possibilities, we crossed the *ets-5(tm1734)* strain into a mutant lacking the EAT-2 ligand-gated ion channel that has been used to model dietary restriction in previous studies (35, 36). The EAT-2 channel is required for rapid pharyngeal pumping on food, and as such, the rate of pumping in *eat-2(ad465)* mutant animals fed on *E. coli* bacteria was only ∼15% that of WT animals. Consequently, *eat-2(ad465)* mutants stored less fat and explored more compared with WT animals (37) (Fig. 4*B*). We also found that the *eat-2(ad465)* mutation fully suppressed the *ets-5(tm1734)* exploration defect (Fig. 4*B*). Taken together, these data show that decreasing food intake can reverse the reduced exploratory behavior of *ets-5* mutant animals. A possible explanation for this shift in behavior could be that *ets-5* controls the level of an internal satiety signal, and that a reduction of food cues stimulates exploratory behavior to enable optimal foraging.

***ets-5* Mutants Exhibit Increased Fat Storage.** What could be the satiety signal in *ets-5* mutant animals that causes reduced exploration? We hypothesized that loss of *ets-5* may cause increased fat storage, and that the resulting enhanced satiety might thus trigger quiescence. Indeed, it has been noted that quiescent animals often have a dark intestine, an indicator of increased fat storage (1). In *C. elegans*, fat storage can be assayed by staining fixed worms with the lipophilic dyes Nile Red and Oil Red O (37, 38). We stained *ets-5* mutant animals using both dyes and found that loss of *ets-5* caused enhanced fat storage compared with WT animals (Fig. 5*A* and Fig. S5*A*). The increase in body fat was not accompanied by an enhanced rate of pharyngeal pumping (Fig. S5*B*), suggesting that a shift in metabolism, rather than increased feeding, is responsible for the increased body fat phenotype of *ets-5* mutant animals.

Based on our finding that transgenic expression of *ets-5* in the ASG and BAG neurons rescued the *ets-5* mutant defect in exploratory behavior (Fig. 2*B*), we asked whether such neuron-specific expression could rescue the excess fat phenotype of the *ets-5(tm1734)* mutant. Using Oil Red O staining, we found that expression of *ets-5* cDNA in the ASG and BAG neurons reduced the levels of fat in *ets-5* mutant animals (Fig. 5*B*). These data suggest that increased fat in *ets-5* mutant animals causes a reduction in exploratory behavior.

To more directly investigate whether increased fat storage in *ets-5* mutant animals causes reduced exploration, we decreased body fat levels in the intestine by RNAi of *pod-2* (encoding an acetyl-CoA carboxylase that produces malonyl CoA, a crucial precursor of fatty acid synthesis) and *elo-2* (encoding a palmitic acid elongase that converts C16:0 fatty acids to C18:0 fatty acids) (39–41). We found that *pod-2* and *elo-2* RNAi partially suppressed

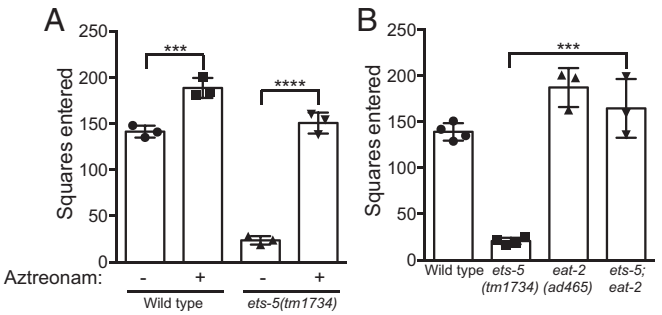

Fig. 4. Suppression of *ets-5* mutant defects by malnutrition. (*A*) Cultivation of WT animals with aztreonam-treated OP50 *E. coli* increases exploratory behavior. In addition, the exploratory defect of *ets-5(tm1734)* mutant animals is fully suppressed when animals are grown on this inedible food source. At least three independent replicates are shown ($n > 20$ per replicate). $^{***}P < 0.001$, $^{****}P < 0.0001$, ANOVA with Tukey's multiple comparisons test. (*B*) *eat-2(ad465)* mutant animals exhibit increased exploration compared with WT animals grown on OP50 *E. coli*. The exploratory defect of *ets-5(tm1734)* mutant animals is fully suppressed when *eat-2* is mutated. At least three independent replicates are shown ($n > 20$ per replicate). $^{***}P < 0.001$, ANOVA with Tukey's multiple comparisons test.

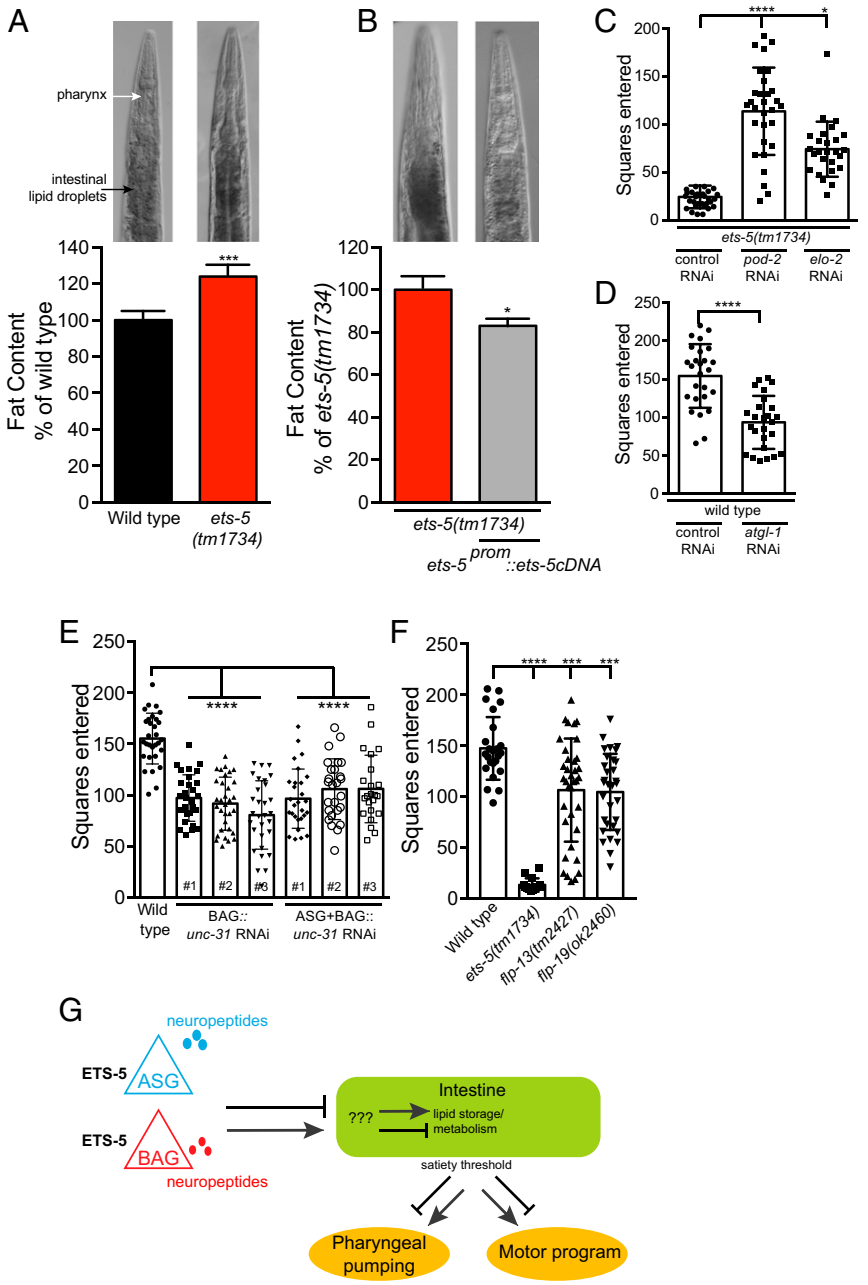

Fig. 5. Intestinal fat levels correlate with quiescence in *ets-5* mutant animals. (*A*, *Top*) Representative images of WT (*Left*) and the *ets-5(tm1734)* mutant (*Right*) fixed and stained with Oil Red O. Fat deposition in intestinal cells is visible as stained lipid droplets (black arrow). Animals are oriented facing upward, with the pharynx (white arrow) at the anterior. (*A*, *Bottom*) Fat content quantified for each genotype and presented as a percentage of WT animals ± SEM. $n = 45$. ***$P <$ 0.001, *t* test. (*B*) Expression of *ets-5* cDNA controlled by the 4-kb *ets-5* promoter (BAG- and ASG-expressed) reduces intestinal fat levels of *ets-5(tm1734)* mutant animals. (*Top*) Representative images of an *ets-5(tm1734)* mutant animal (*Left*) and an *ets-5(tm1734)* mutant animal carrying the *ets-5^{prom}::ets-5 cDNA* rescuing array (*Right*) fixed and stained with Oil Red O. (*Bottom*) Fat content quantified and presented as a percentage of *ets-5(tm1734)* mutant animals ± SEM. $n = 36$. *$P < 0.01$, *t* test. Transgenic rescue line 3 from Fig. 2*B* was used for this analysis. (*C*) *pod-2* or *elo-2* RNAi knockdown suppresses the exploratory defect of *ets-5(tm1734)* mutant animals. L4440 (empty RNAi vector)-containing bacteria served as a control. $n >20$. *$P < 0.03$, ****$P < 0.0001$, ANOVA with Tukey's multiple comparisons test. (*D*) *atgl-1* RNAi knockdown reduces exploration of WT animals. L4440 (empty RNAi vector)-containing bacteria served as a control. $n >26$. ****$P < 0.0001$, Mann–Whitney *U* test. (*E*) RNAi knockdown of *unc-31* in the BAG (*gcy-33* promoter) or BAG and ASG neurons (*ets-5* promoter) reduces exploratory behavior of WT animals. $n >23$. ****$P < 0.001$, ANOVA with Tukey's multiple comparisons test. # refers to independent transgenic lines. (*F*) Deletion mutants of the FLP-13 and FLP-19 neuropeptides cause reduced exploratory behavior. WT and *ets-5(tm1734)* animals served as controls. $n >15$. ****$P < 0.0001$, ***$P < 0.001$, ANOVA with Tukey's multiple comparisons test. (*G*) ETS-5 acts in the ASG and BAG neurons to regulate intestinal fat levels and exploratory behavior using predominantly neuropeptidergic signaling. We propose that fat levels affect organismal activity, where increased fat suppresses the feeding program (pharyngeal pumping) and motor program (exploratory locomotion). An intestinal satiety threshold maintains the appropriate level of activity for specific environmental conditions.

the defect in exploratory behavior of *ets-5* mutant animals (Fig. 5*C*), suggesting that the increased intestinal fat level in *ets-5* mutant animals causes the change in behavior.

To further investigate the link between fat storage and exploration, we increased intestinal fat levels in WT animals by performing RNAi against *atgl-1* (encoding an adipocyte triglyceride

lipase) (42). We found that *atgl-1* RNAi caused a reduction in exploratory behavior (Fig. 5*D*). Therefore, our data indicate that internal fat stores can be interpreted by *C. elegans* to modify exploratory behavior.

We have shown that exploratory behavior is modulated by genetic perturbations that regulate fat storage in *C. elegans* (Fig. 5). We next asked whether a change in diet could directly modify exploratory behavior. High-glucose diets in humans are closely linked to obesity (43). Likewise, glucose supplementation to the *C. elegans* diet caused a significant rise in fat storage, likely by altering the quality of bacterial food grown on glucose (44) (Fig. S5 *C* and *D*). Therefore, we investigated whether diet-induced fat storage also might affect exploratory behavior in WT animals by feeding worms with bacteria supplied with a high-glucose diet. As expected, we found that a high-glucose diet reduced the exploratory behavior of WT animals (Fig. S5*E*), as demonstrated by a decrease in the proportion of animals roaming (from 21% to 11%) and an increase in the proportion of those in quiescence (from 4% to 10%). This behavioral defect could be reversed after recovery on food with no glucose supplement (Fig. S5*E*), which is associated with decreased fat staining (Fig. S5*F*). These data indicate that the exploratory behavior of *C. elegans* is dynamic and responsive to internally generated satiety cues, most likely from the intestine.

Neuropeptide Signaling Contributes to the Control of Exploratory Behavior. Because the *C. elegans* intestine is not directly innervated, communication between the ASG and BAG neurons and the intestine most likely occurs through the action of neuropeptides. To test this hypothesis, we performed neuron-specific RNAi against *unc-31*, which encodes a calcium-dependent activator protein for secretion that is required for neuropeptide release (45). We found that both BAG-specific (*gcy-33* promoter) and ASG- and BAG-specific (*ets-5* promoter) knockdown of *unc-31* reduced the exploratory behavior of WT animals (Fig. 5*E*). The reduced exploratory capacity of ASG and BAG knockdown was similar to that of BAG knockdown alone, suggesting that the role of neuropeptides in the control of exploration may originate predominantly from the BAG neurons.

The transcriptional targets of ETS-5 in the ASG and BAG neurons have not been fully described; however, previous studies have shown that specific FMRFamide-related neuropeptides, expressed in the BAG neurons (FLP-13 and FLP-19), are regulated by ETS-5 (26, 27). Therefore, we examined the behavior of mutant strains lacking these neuropeptides, and found that loss of both *flp-13* and *flp-19* caused a partial decrease in exploratory capacity. Taken together, our findings show that the ETS-5 TF acts in the ASG and BAG neurons to control satiety-regulated behavioral states in *C. elegans*, most likely through the action of multiple neuropeptides (Fig. 5*G*).

Discussion

Satiety signals from the gastrointestinal tract and adiposity indicators from adipose tissue control appetite in mammals. Hypothalamic regions in the mammalian brain assimilate such information to enable the formulation of appropriate food-related behavioral responses. In *C. elegans*, as in mammals, satiety results in quiescence, which is reminiscent of postprandial somnolence. Here we report that the conserved ETS-5 TF regulates quiescence in *C. elegans* through the control of satiety. WT *C. elegans* exposed to low-quality food minimally entered quiescence owing to a lack of satiety, a behavior controlled by ETS-5, given that loss of this TF caused enhanced quiescence under the same conditions. As such, we propose that ETS-5 is required for setting the "satiety quotient" in *C. elegans*. In support of this hypothesis, we found that reducing fatty acid synthesis in the intestine was sufficient to suppress the *ets-5* mutant defects in exploratory behavior.

We found that when *ets-5* mutant animals were exposed to inedible food or their feeding was genetically impeded, their exploratory behavior resembled that of WT animals. This reversion of behavior is rapid, indicating that *ets-5* mutant animals can perceive and respond to their environment when challenged with low concentrations of food in their pharynx. Therefore, the ability to perceive the presence of low-value nutritional food through mechanosensory and chemosensory cues (34) is intact in *ets-5* mutant animals. These findings suggest that signals reporting the internal metabolic state of the animals (satiety) can be overridden by indicators of poor food influx into the mouth, most likely through neuronal signaling. This would be a potential means of anticipating starvation that would enable animals to rapidly relocate to more optimal environments. Given that *C. elegans* lose approximately 70% of their body fat within 2–3 h of fasting (40), the rapid reversal of exploratory behavior is an important survival mechanism in these animals.

We have shown that satiety-induced quiescence can be promoted by a diet that causes excessive storage of fat in *C. elegans*. Remarkably, we found that the behavioral consequence of high fat stores (quiescence) in *C. elegans* can be reversed after a few hours on a regular bacterial diet. This suggests that satiety-induced quiescence caused by excess fat may be used as a model to identify molecular and neuronal mechanisms that control interactions between the gut and nervous system.

Our genetic data and the neuronal circuitry work of others (2) indicate the existence of a complex network of mostly non-overlapping neuronal signaling pathways (5-HT, PDF, cGMP) that control exploratory behavior. This is not surprising, considering that the ephemeral habitat of *C. elegans* (46) requires a sophisticated mechanism for perceiving complex external food cues and integrating this information with the internal metabolic state. We have identified a TF, ETS-5, as an important regulator of exploratory behavior, promoting roaming of *C. elegans* while inhibiting quiescence. As such, ETS-5 may be considered an arousal factor; our data suggest that ETS-5 acts in the same pathway as PDFR-1 in this regard. Given that PDF signaling also acts in *Drosophila* to promote waking states (47), it will be interesting to establish whether PDF in the fruit fly acts in conjunction with an ETS TF to control wakefulness.

Our genetic analysis also identified a role for MOD-1–directed 5-HT signaling in quiescence. Loss of MOD-1 caused complete suppression of satiety-induced quiescence in *ets-5* mutant animals, suggesting that when animals are sated, modification of serotoninergic signaling can still regulate quiescence. The significance of this finding in *C. elegans* is unclear; nonetheless, there appears to be a conserved role for 5-HT in the regulation of feeding behavior in other systems (48).

We have shown that the ASG and BAG neurons are important for the regulation of exploratory behavior. Previously, the ASG neurons were shown to regulate dauer formation and longevity, in addition to the detection of food or food breakdown products (49–51). The ASG neurons are also able to act in stress conditions when they are recruited to a novel neuronal circuit to enable an escape response (52). In contrast, the BAG neurons function to detect changes in oxygen and carbon dioxide in the environment and to coordinate behavioral responses according to changes in environmental gas status (26, 53–56). Our behavioral state analysis shows that the ASG and BAG neurons are both important for the inhibition of quiescence under standard laboratory conditions, whereas the ASG neurons potentially play a more major role in the inhibition of roaming behavior.

Owing to the absence of intestinal innervation in *C. elegans*, communication between the nervous system and intestine most likely occurs through the action of neuropeptides. Indeed, we found that disrupted neuropeptide release from the ASG and BAG neurons partially reduces exploratory capacity, as does loss of specific neuropeptides from the BAG neurons. Future work

should concentrate on understanding the molecular mechanism through which ETS-5 controls body fat storage/metabolism through the action of neuropeptides, and how satiety signals control locomotion and feeding. Multiple ETS TFs have been linked to obesity in humans (57–60), and thus the important role of the ETS-5 TF that we describe here may be conserved in higher organisms as well.

Materials and Methods

***C. elegans* Maintenance.** All *C. elegans* strains were cultured on NGM plates at 20 °C as described previously unless stated otherwise (61). All strains generated and used in this study are described in *SI Materials and Methods*.

Exploration Assay. Exploration assays were performed as reported previously (2) and described in detail in *SI Materials and Methods*. Single OP50 *E. coli* colonies were inoculated in 400 mL of LB and incubated at 37 °C overnight for 16 h without shaking. Worms were grown in uncrowded conditions to the L4 stage. Individual L4 animals were then placed in the center of 55-mm NGM plates uniformly seeded with 500 μL of OP50 *E. coli* bacteria that had been grown for 48 h at 20 °C. After a 16-h period of exploration at 20 °C, the worms were removed, plates were superimposed on a grid of 3-mm squares, and the number of squares entered by worm tracks was counted manually. The investigator was blinded to genotype, and experiments were repeated at least three times.

ACKNOWLEDGMENTS. We thank members of the R.P. laboratory, Baris Tursun, and Luisa Cochella for comments on the manuscript. Some strains used in this study were provided by the *Caenorhabditis* Genetics Center, which is funded by the National Institutes of Health's Office of Research Infrastructure Programs (Grant P40 OD010440), and by Shohei Mitani at the National Bioresource Project (Japan), Cori Bargmann, Mario de Bono, David Raizen, and Manuel Zimmer. This work was supported by a grant from the European Research Council (ERC Starting Grant 260807), a Monash University Biomedicine Discovery Fellowship, and a Victorian Endowment for Science, Knowledge and Innovation fellowship (VIF 23) (to R.P.).

1. You YJ, Kim J, Raizen DM, Avery L (2008) Insulin, cGMP, and TGF-beta signals regulate food intake and quiescence in *C. elegans*: A model for satiety. *Cell Metab* 7(3): 249–257.
2. Flavell SW, et al. (2013) Serotonin and the neuropeptide PDF initiate and extend opposing behavioral states in *C. elegans*. *Cell* 154(5):1023–1035.
3. Ben Arous J, Laffont S, Chatenay D (2009) Molecular and sensory basis of a food related two-state behavior in *C. elegans*. *PLoS One* 4(10):e7584.
4. Shtonda BB, Avery L (2006) Dietary choice behavior in *Caenorhabditis elegans*. *J Exp Biol* 209(Pt 1):89–102.
5. Yamanaka A, et al. (2003) Hypothalamic orexin neurons regulate arousal according to energy balance in mice. *Neuron* 38(5):701–713.
6. Linford NJ, Chan TP, Pletcher SD (2012) Re-patterning sleep architecture in *Drosophila* through gustatory perception and nutritional quality. *PLoS Genet* 8(5):e1002668.
7. Dewasmes G, Duchamp C, Minaire Y (1989) Sleep changes in fasting rats. *Physiol Behav* 46(2):179–184.
8. Antin J, Gibbs J, Holt J, Young RC, Smith GP (1975) Cholecystokinin elicits the complete behavioral sequence of satiety in rats. *J Comp Physiol Psychol* 89(7):784–790.
9. Fujiwara M, Sengupta P, McIntire SL (2002) Regulation of body size and behavioral state of *C. elegans* by sensory perception and the EGL-4 cGMP-dependent protein kinase. *Neuron* 36(6):1091–1102.
10. Hetherington AW, Ranson SW (1940) Hypothalamic lesions and adiposity in the rat. *Anat Rec* 78(2):149–172.
11. Schwartz MW, Woods SC, Porte D, Jr, Seeley RJ, Baskin DG (2000) Central nervous system control of food intake. *Nature* 404(6778):661–671.
12. Kageyama H, et al. (2012) Neuronal circuits involving neuropeptide Y in hypothalamic arcuate nucleus-mediated feeding regulation. *Neuropeptides* 46(6):285–289.
13. Sclafani A (1989) Dietary-induced overeating. *Ann N Y Acad Sci* 575:281–289; discussion 290-281.
14. Pérez C, Fanizza LJ, Sclafani A (1999) Flavor preferences conditioned by intragastric nutrient infusions in rats fed chow or a cafeteria diet. *Appetite* 32(1):155–170.
15. Gallagher T, You YJ (2014) Falling asleep after a big meal: Neuronal regulation of satiety. *Worm* 3:e27938.
16. Hart AH, Reventar R, Bernstein A (2000) Genetic analysis of ETS genes in *C. elegans*. *Oncogene* 19(55):6400–6408.
17. Hollenhorst PC, McIntosh LP, Graves BJ (2011) Genomic and biochemical insights into the specificity of ETS transcription factors. *Annu Rev Biochem* 80:437–471.
18. Macleod K, Leprince D, Stehelin D (1992) The ets gene family. *Trends Biochem Sci* 17(7):251–256.
19. Karim FD, et al. (1990) The ETS-domain: A new DNA-binding motif that recognizes a purine-rich core DNA sequence. *Genes Dev* 4(9):1451–1453.
20. Sementchenko VI, Watson DK (2000) Ets target genes: Past, present and future. *Oncogene* 19(55):6533–6548.
21. Wei GH, et al. (2010) Genome-wide analysis of ETS-family DNA-binding in vitro and in vivo. *EMBO J* 29(13):2147–2160.
22. Flames N, Hobert O (2009) Gene regulatory logic of dopamine neuron differentiation. *Nature* 458(7240):885–889.
23. Schmid C, Schwarz V, Hutter H (2006) AST-1, a novel ETS-box transcription factor, controls axon guidance and pharynx development in *C. elegans*. *Dev Biol* 293(2): 403–413.
24. Tan PB, Lackner MR, Kim SK (1998) MAP kinase signaling specificity mediated by the LIN-1 Ets/LIN-31 WH transcription factor complex during *C. elegans* vulval induction. *Cell* 93(4):569–580.
25. Thyagarajan B, et al. (2010) ETS-4 is a transcriptional regulator of life span in *Caenorhabditis elegans*. *PLoS Genet* 6(9):e1001125.
26. Brandt JP, et al. (2012) A single gene target of an ETS-family transcription factor determines neuronal CO_2-chemosensitivity. *PLoS One* 7(3):e34014.
27. Guillermin ML, Castelletto ML, Hallem EA (2011) Differentiation of carbon dioxide-sensing neurons in *Caenorhabditis elegans* requires the ETS-5 transcription factor. *Genetics* 189(4):1327–1339.
28. Ray RS, et al. (2011) Impaired respiratory and body temperature control upon acute serotonergic neuron inhibition. *Science* 333(6042):637–642.
29. Hendricks TJ, et al. (2003) Pet-1 ETS gene plays a critical role in 5-HT neuron development and is required for normal anxiety-like and aggressive behavior. *Neuron* 37(2):233–247.
30. Ciarleglio CM, Resuehr HE, Axley JC, Deneris ES, McMahon DG (2014) Pet-1 deficiency alters the circadian clock and its temporal organization of behavior. *PLoS One* 9(5): e97412.
31. Ullrich M, et al. (2011) Identification of SPRED2 (sprouty-related protein with EVH1 domain 2) as a negative regulator of the hypothalamic-pituitary-adrenal axis. *J Biol Chem* 286(11):9477–9488.
32. Budry L, Couture C, Balsalobre A, Drouin J (2011) The Ets factor Etv1 interacts with Tpit protein for pituitary pro-opiomelanocortin (POMC) gene transcription. *J Biol Chem* 286(28):25387–25396.
33. Chelur DS, Chalfie M (2007) Targeted cell killing by reconstituted caspases. *Proc Natl Acad Sci USA* 104(7):2283–2288.
34. Gruninger TR, Gualberto DG, Garcia LR (2008) Sensory perception of food and insulin-like signals influence seizure susceptibility. *PLoS Genet* 4(7):e1000117.
35. Raizen DM, Lee RY, Avery L (1995) Interacting genes required for pharyngeal excitation by motor neuron MC in *Caenorhabditis elegans*. *Genetics* 141(4):1365–1382.
36. Lakowski B, Hekimi S (1998) The genetics of caloric restriction in *Caenorhabditis elegans*. *Proc Natl Acad Sci USA* 95(22):13091–13096.
37. Brooks KK, Liang B, Watts JL (2009) The influence of bacterial diet on fat storage in *C. elegans*. *PLoS One* 4(10):e7545.
38. Soukas AA, Kane EA, Carr CE, Melo JA, Ruvkun G (2009) Rictor/TORC2 regulates fat metabolism, feeding, growth, and life span in *Caenorhabditis elegans*. *Genes Dev* 23(4):496–511.
39. Salway JG (1999) Metabolism at a Glance (Blackwell Science, Oxford, UK) 2nd Ed, p 111.
40. Witham E, et al. (2016) *C. elegans* body cavity neurons are homeostatic sensors that integrate fluctuations in oxygen availability and internal nutrient reserves. *Cell Rep* 14(7):1641–1654.
41. Kniazeva M, Crawford QT, Seiber M, Wang CY, Han M (2004) Monomethyl branched-chain fatty acids play an essential role in *Caenorhabditis elegans* development. *PLoS Biol* 2(9):E257.
42. Noble T, Stieglitz J, Srinivasan S (2013) An integrated serotonin and octopamine neuronal circuit directs the release of an endocrine signal to control *C. elegans* body fat. *Cell Metab* 18(5):672–684.
43. Brand-Miller JC, Holt SH, Pawlak DB, McMillan J (2002) Glycemic index and obesity. *Am J Clin Nutr* 76(1):281S–285S.
44. Garcia AM, et al. (2015) Glucose induces sensitivity to oxygen deprivation and modulates insulin/IGF-1 signaling and lipid biosynthesis in *Caenorhabditis elegans*. *Genetics* 200(1):167–184.
45. Sieburth D, Madison JM, Kaplan JM (2007) PKC-1 regulates secretion of neuropeptides. *Nat Neurosci* 10(1):49–57.
46. Félix MA, Braendle C (2010) The natural history of *Caenorhabditis elegans*. *Curr Biol* 20(22):R965–R969.
47. Sehgal A, Mignot E (2011) Genetics of sleep and sleep disorders. *Cell* 146(2):194–207.
48. Versteeg RI, Serlie MJ, Kalsbeek A, la Fleur SE (2015) Serotonin, a possible intermediate between disturbed circadian rhythms and metabolic disease. *Neuroscience* 301:155–167.
49. Bargmann CI, Horvitz HR (1991) Control of larval development by chemosensory neurons in *Caenorhabditis elegans*. *Science* 251(4998):1243–1246.
50. Bargmann CI, Horvitz HR (1991) Chemosensory neurons with overlapping functions direct chemotaxis to multiple chemicals in *C. elegans*. *Neuron* 7(5):729–742.
51. Alcedo J, Kenyon C (2004) Regulation of *C. elegans* longevity by specific gustatory and olfactory neurons. *Neuron* 41(1):45–55.
52. Pocock R, Hobert O (2010) Hypoxia activates a latent circuit for processing gustatory information in *C. elegans*. *Nat Neurosci* 13(5):610–614.
53. Zimmer M, et al. (2009) Neurons detect increases and decreases in oxygen levels using distinct guanylate cyclases. *Neuron* 61(6):865–879.
54. Brandt JP, Ringstad N (2015) Toll-like receptor signaling promotes development and function of sensory neurons required for a *C. elegans* pathogen-avoidance behavior. *Curr Biol* 25(17):2228–2237.

55. Hallem EA, Sternberg PW (2008) Acute carbon dioxide avoidance in *Caenorhabditis elegans*. *Proc Natl Acad Sci USA* 105(23):8038–8043.
56. Bretscher AJ, et al. (2011) Temperature, oxygen, and salt-sensing neurons in *C. elegans* are carbon dioxide sensors that control avoidance behavior. *Neuron* 69(6):1099–1113.
57. Thorleifsson G, et al. (2009) Genome-wide association yields new sequence variants at seven loci that associate with measures of obesity. *Nat Genet* 41(1):18–24.
58. Willer CJ, et al.; Wellcome Trust Case Control Consortium; Genetic Investigation of Anthropometric Traits Consortium (2009) Six new loci associated with body mass index highlight a neuronal influence on body weight regulation. *Nat Genet* 41(1): 25–34.
59. Birsoy K, et al. (2011) Analysis of gene networks in white adipose tissue development reveals a role for ETS2 in adipogenesis. *Development* 138(21):4709–4719.
60. Wang F, Tong Q (2008) Transcription factor PU.1 is expressed in white adipose and inhibits adipocyte differentiation. *Am J Physiol Cell Physiol* 295(1):C213–C220.
61. Brenner S (1974) The genetics of *Caenorhabditis elegans*. *Genetics* 77(1):71–94.
62. Timmons L, Fire A (1998) Specific interference by ingested dsRNA. *Nature* 395(6705): 854.
63. Hobert O (2002) PCR fusion-based approach to create reporter gene constructs for expression analysis in transgenic *C. elegans*. *Biotechniques* 32(4):728–730.
64. Tsunozaki M, Chalasani SH, Bargmann CI (2008) A behavioral switch: cGMP and PKC signaling in olfactory neurons reverses odor preference in *C. elegans*. *Neuron* 59(6): 959–971.
65. Ramot D, Johnson BE, Berry TL, Jr, Carnell L, Goodman MB (2008) The Parallel Worm Tracker: A platform for measuring average speed and drug-induced paralysis in nematodes. *PLoS One* 3(5):e2208.
66. Pino EC, Webster CM, Carr CE, Soukas AA (2013) Biochemical and high-throughput microscopic assessment of fat mass in *Caenorhabditis elegans*. *J Vis Exp* 73:50180.
67. Bargmann CI, Avery L (1995) Laser killing of cells in *Caenorhabditis elegans*. *Methods Cell Biol* 48:225–250.

Supporting Information

Juozaityte et al. 10.1073/pnas.1610673114

SI Materials and Methods

***C. elegans* Transgenics.** All constructs were injected into young adult hermaphrodites as simple arrays. *myo-2^{prom}::dsRed* (5 ng μL^{-1}) or *elt-2^{prom}::gfp* (5 ng μL^{-1}) was used as a coinjection marker.

Nematode Strains. The following *C. elegans* strains were used: N2 (Bristol strain, WT), RJP235 *ets-5(tm1734)*, RJP1532 (*ets-5(tm866)*, RJP1892 *ets-5(tm1734); rpEx794(ets-5* WRM061dH11 fosmid), RJP3085 *rpEx1520(ets-5^{prom}::mCherry)*, PY1512 *ops-1^{prom}::GFP*, RJP3038 *ets-5(tm1734); rpEx1507(ets-5$^{prom(4kb)}$::ets-5cDNA),* RJP3069 *ets-5(tm1734); rpEx1513(ets-5$^{prom(4kb)}$::ets-5cDNA),* RJP3071 *ets-5(tm1734); rpEx1515(ets-5$^{prom(4kb)}$::ets-5cDNA),* CX11697 *kyIs536(flp-17^{prom}::caspase p17::SL2::gfp elt-2^{prom}::gfp); kyIs538(glb-5^{prom}::caspase p12::SL2::gfp elt-2^{prom}::dsRed)*, MT9668 *mod-1(ok103),* RJP1893 *mod-1(ok103); ets-5(tm1734),* VC2609 *pdfr-1(ok3425)*, RJP1791 *pdfr-1(ok3425); ets-5(tm1734)*, MT1072 *egl-4(n479),* RJP1568 *egl-4(n479); ets-5(tm1734)*, DA465 *eat-2(ad465)*, RJP1911 *eat-2(ad465); ets-5(tm1734)*, NQ602 *flp-13(tm2427)*, RJP3505 *flp-19(ok2460)*, MT14525 *gcy-9(n4470)*, RJP3497 *gcy-31(ok296); gcy-33(ok232)*, and RJP3496 *gcy-31(ok296) gcy-9(n4470); gcy-33(ok232).*

Neuron-Specific RNAi. The 4-kb *ets-5* promoter, which drives expression in the ASGL/R and BAGL/R neurons, was used to express the *ets-5* snap-back construct. The snap-back construct with inverted repeats (IR) of 505 bp from the *ets-5* coding sequence was generated from two plasmids. The first plasmid contained *ets-5* promoter driving the 505-bp *ets-5* sequence in sense orientation. The second plasmid contained 505bp of *ets-5* sequence in the antisense orientation and the *unc-54* 3′UTR. The sequence from the first plasmid containing *ets-5^{prom}* (505bp *ets-5* coding DNA) was then PCR amplified and fused to the sequence containing 505bp antisense sequence and *unc-54* 3′UTR from the second plasmid. Correctly amplified snap-back products were confirmed by agarose gel electrophoresis.

RNAi by Feeding. RNA interference was performed using the feeding method as described previously (62). Larvae were placed on IPTG-containing plates seeded with *E. coli* [(HT115(DE3)] expressing dsRNA of specific genes studied or the vector-only control (L4440).

Microscopy. Animals were anesthetized with 20 mM NaN_3 on 5% agarose pads, and images were obtained with an Axio Imager M2 fluorescence microscope and Zen software (Zeiss).

Molecular Cloning. The *ets-5* transcriptional reporter was generated by PCR fusion (63). The full intergenic upstream region of *ets-5* (4 kb) was PCR-amplified and then fused to the sequence encoding the *mCherry* reporter and *unc-54* 3′UTR. Rescue constructs were generated by cloning the promoter and cDNA sequences into the pPD49.26 expression vector (Fire Lab *C. elegans* Vector Kit, Addgene). The oligonucleotides used in this study are available on request.

Behavioral State Assay. The behavioral state of individual animals (roaming, dwelling, or quiescent) was performed essentially as described previously (1). Before removing the individual worms from the exploration assays (see above), we analyzed their behavioral state at 20 °C. The exploration plates were placed individually on a microscope with the lid on and left for 15 s, after which pharyngeal pumping and movement were observed for 10 s (under 45× magnification using an Olympus SX61 stereomicroscope with white light). An animal that exhibited continuous forward movement was scored as roaming, an animal that turned frequently or was stationary but pumped its pharynx was scored as dwelling, and an animal that did not move or pump its pharynx was deemed quiescent.

Gustatory Behavioral Assay. The response to salt gradients was assayed as described previously (52). In brief, 10 mL of buffered agar (20 g L^{-1} agar, 1 mM $CaCl_2$, 1 mM $MgSO_4$, and 5 mM KPO_4) was poured into 10-cm diameter Petri dishes. To establish a salt gradient, at 12–16 h before the assay, 10 μL of 2.5 M NaCl solution adjusted to pH 6 was applied to the attractant spot, and 10 μL of ddH_2O was applied to the control spot. Another 4 μL of 2.5M NaCl solution or water was added to the same spots at 4 h before the assay. A 1-μL drop of 1 M sodium azide was applied to both the attractant and control spots 10 min before the assay to immobilize worms that reached these areas. Synchronized adult animals were washed three times with CTX solution (1 mM $CaCl_2$, 1 mM $MgSO_4$, and 5 mM KPO_4), and 100–200 worms were placed in the center of the assay plate in a minimal volume of buffer. Animals were permitted to navigate the agar surface for 1 h, after which the assay plates were placed at 4 °C overnight. The distribution of animals across the plate was then determined, and a chemotaxis index was calculated as the number of animals at the NaCl area minus the number of animals at the control area, divided by the total number of animals. Animals that did not leave the central origin were discriminated in the analysis. Gustatory behavioral assays were performed on three separate days with three assays per day.

Olfactory Behavioral Assay. Olfactory assays were prepared in a similar manner as the gustatory assays, except that worms were washed with S-basal buffer. In addition, the odors (1:1,000 2,3-pentanedione or 1:100 diacetyl) or the control (100% ethanol) were placed on opposite sides of the assay plate immediately after the worms were transferred to the center of the plate. The plates were then sealed with parafilm, and after 1 h, the assay plates were placed at 4 °C overnight and then scored in the same way as for the gustatory behavioral assays. Olfactory behavioral assays were performed on three separate days with three assays per day.

Oxygen-Sensing Behavioral Assay. WT and *ets-5* mutant animals were starved for 1 h and then transferred to 14-cm NGM plates containing a 56 × 56-mm arena of Whatman filter paper soaked in 20 mM $CuCl_2$. Between 80 and 120 animals were used in a single experiment. Each experimental condition was repeated three times. A custom-made transparent Plexiglas chamber with a flow volume of 60 × 60 × 0.7 mm was placed onto the assay arena, and the animals were accustomed to a gas flow of 100 mL/min containing 21% (vol/vol) O_2 for 5 min. The animals were stimulated for 6 min with 10% or 21% O_2 and 0% CO_2. In all conditions, the gas compositions were balanced with N_2. Gases were mixed by red-y gas mixing units (Vögtlin Instruments) and controlled by LabView software. Recordings were illuminated with flat red LED lights and made at 3 fps on a 4-megapixel CCD camera (Jai), using Streampix software (Norpix). For movie analysis, MatLab-based image processing and tracking scripts were used as described previously (64, 65). The resultant trajectories were used to calculate instantaneous speed during continuous forward movements (1-s binning).

Pharyngeal Pumping Assay. Five L4 larvae were placed on a lawn of OP50 *E. coli*. The following day, pharyngeal pumping of the resultant 1-d-old adults was counted over a 30-s period. The

recorded number of pumps was doubled to generate a "pumps per minute" value. The experiment was repeated on three separate days.

Oil Red O Staining. Oil Red O staining was performed essentially as described previously (42) with the following amendments: animals were fixed for 5 min with 4% formaldehyde and 0.5% β-mercaptoethanol before the freeze-thaw cycles. In each experiment, ∼4,000 animals were fixed and stained. Each experiment was repeated at least three times. WT and *ets-5(tm1734)* animals were included in each independent experiment as controls.

Nile Red Staining. The fixation Nile Red staining protocol was as described previously (66). In each experiment, ∼4,000 animals were fixed and stained. Each experiment was repeated at least three times. WT animals were included in each independent experiment as controls.

Quantification of Fat Storage. To quantify the levels of fat, images of Oil Red O- and Nile Red-stained worms were obtained using a Zeiss Axio Imager M2, and images were quantified with ImageJ software. Lipid droplet staining in the first four pairs of intestinal cells (Oil Red O) or last four pairs of intestinal cells (Nile Red) was quantified. In each experiment, 15–20 animals from each condition were quantified.

Glucose Experiments. Glucose-enriched NGM plates were prepared as described previously (44). In brief, 10-mL NGM plates were fully covered with 400 μL of glucose (D-(+)-glucose; Sigma-Aldrich) of a 1 M stock solution prepared in diH_2O, to reach the desired concentration of 40 mM, and were allowed to dry for 24 h. The next day, 400 μL of *E. coli* OP50 was added on the top of the glucose to cover the entire plate. The bacterial solution was allowed to dry before animals were placed on the plates. All plates were used for experiments within a 7-d period. Two L4 hermaphrodites were transferred onto a glucose plate and allowed to develop to adult worms and lay eggs. The offspring developed on the specific glucose-enriched diet. Exploration tests on OP50 control plates and on glucose-enriched plates were performed using the F_1 generation.

Laser Ablations. Laser ablations were performed as described previously (67), using a Micropoint laser system attached to a Zeiss Axio Imager A2 microscope (Objective EC Plan-Neofluar 100×/1.30 Oil M27). The *ets-5^{prom}::mCherry* strain was used to identify the ASG and BAG neurons, and to confirm that the ablated neurons were killed after the behavioral assays were performed. Ablations were performed on L1-stage animals at 2 h after hatching. Animals were anesthetized on 3% agar pads using 0.05% tetramisole and recovered to OP50-seeded NGM plates before exploration assays. Mock-ablated animals were treated similarly as ablated animals (anesthetized on agar pads for a similar duration), but no ablations were performed.

Genetic Ablations. Genetic ablations were performed using the split caspase system (33). The promoters used to drive the split caspase for ASG ablation were *ops-1^{prom}* (p12 caspase) and *pgcy-21^{prom}* (p17 caspase). Ablations of the BAG neurons and both the ASG and BAG neurons were performed using the same strain (CX11697-*kyIs536*). In this strain, *glb-5^{prom}* drives p12 caspase and *flp-17^{prom}* drives p17 caspase. This strain had previously been used as a BAG ablation strain in multiple studies (26).

We found that when the transgenes were in a heterozygous state, the BAG neurons were killed, and when the transgenes were in a homozygous state, the ASG neurons were also killed. We used this property to our advantage when performing our experiments shown in Fig. 2 *D* and *E*. The *ets-5^{prom}::mCherry* was used to identify the ASG and BAG neurons and to confirm that the ablated neurons were killed after the behavioral assays were performed.

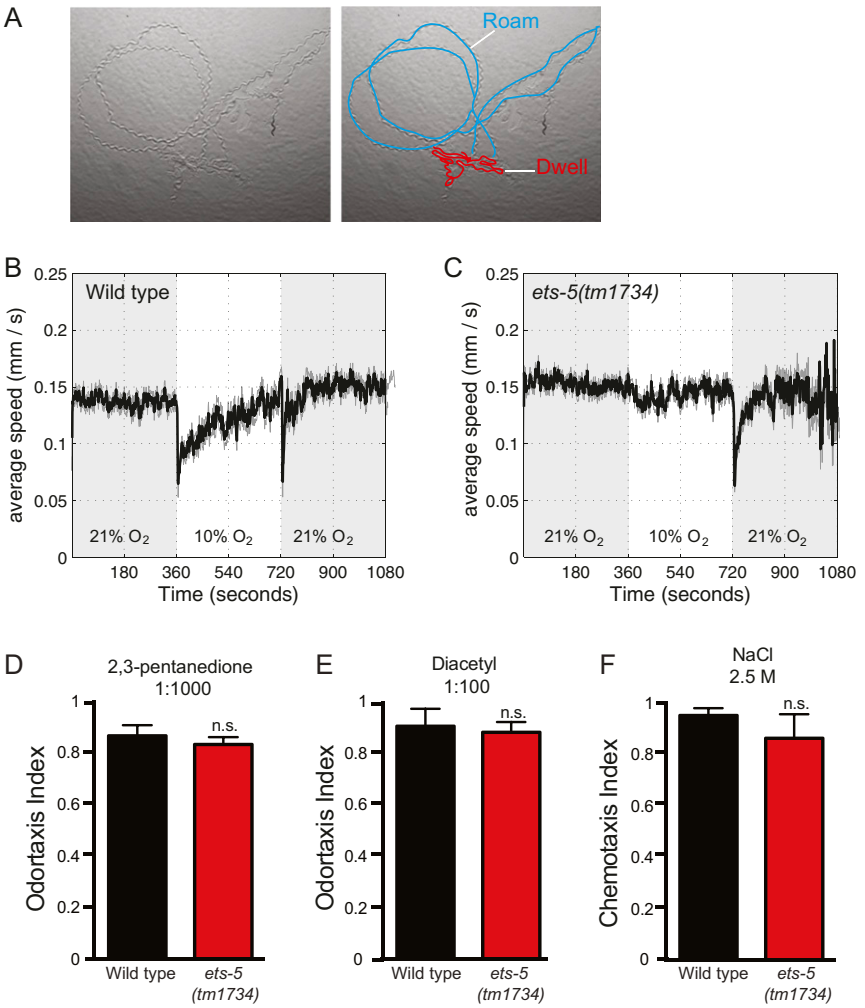

Fig. S1. Behavioral assays (related to Fig. 1). (*A*) Example tracks made by a single L4 worm larva (*Left*) and the same tracks color-coded (*Right*). Short periods of roaming (blue) are punctuated by long periods of dwelling (red). Note that quiescent behavior is not shown here as animals cease locomotion. (*B* and *C*) Locomotion speed of WT (*Left*) and *ets-5(tm1734)* mutant animals (*Right*) during oxygen concentration shifts. Data presented are averages of multiple assays (three or more repetitions). O_2 concentrations were switched between 21% and 10%. Note that *ets-5(tm1734)* mutant animals are unable to sense downsteps in O_2 because of defective BAG specification. (*D–F*) *ets-5(tm1734)* mutant animals are able to respond normally to external sensory cues, sensed by the AWC (2,3-pentanedione), AWA (diacetyl), and ASE (NaCl) neurons. n.s., not significantly different from WT, unpaired *t* test.

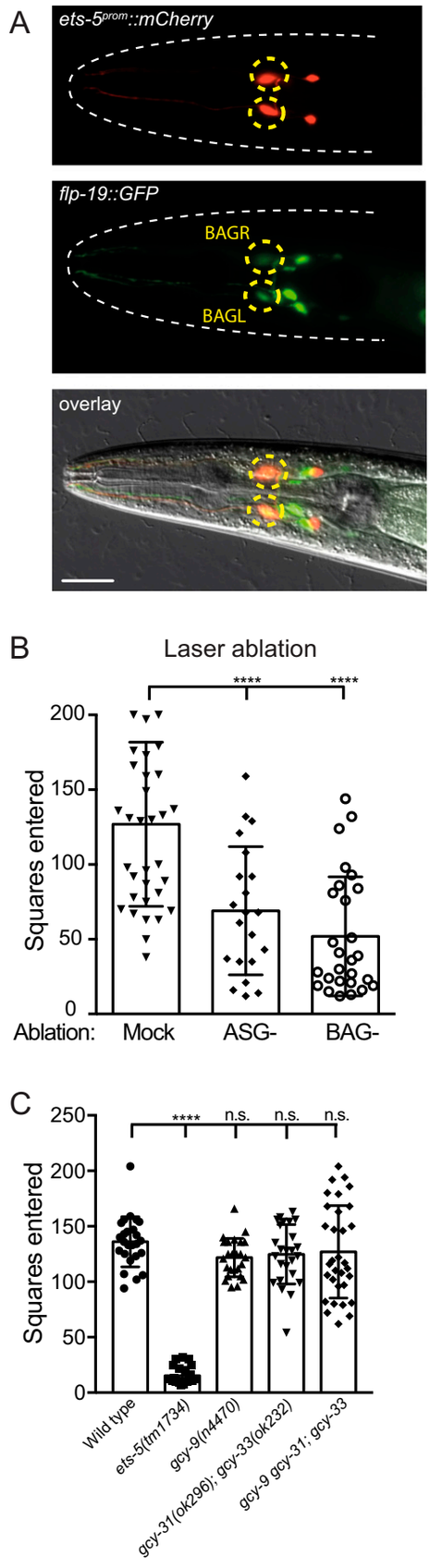

Fig. S2. *ets-5* acts in the ASG and BAG neurons to control exploratory behavior (related to Fig. 2). (*A*) *ets-5*^{prom}*mCherry* reporter (*Top*); *flp-19*^{prom}*::GFP* reporter, expressed in the BAG neurons anteriorly (*Middle*); and overlay with DIC (*Bottom*). Anterior is to the left. (Scale bar: 20 μm.) (*B*) Laser ablation of either the ASG or BAG neurons reduced exploratory behavior of *ets-5*^{prom}*::mCherry*–expressing animals. $n > 21$. ****$P < 0.0001$ compared with mock ablation, ANOVA with Tukey's multiple comparisons test. (*C*) Loss of *gcy-9* (CO_2 sensing), *gcy-31; gcy-33* (O_2 sensing), or *gcy-9 gcy-31; gcy-33* (O_2 and CO_2 sensing) does not disrupt exploratory behavior. WT and *ets-5(tm1734)* animals were used as controls. $n > 25$. ****$P < 0.0001$; n.s., not significantly different from WT animals, ANOVA with Tukey's multiple comparisons test.

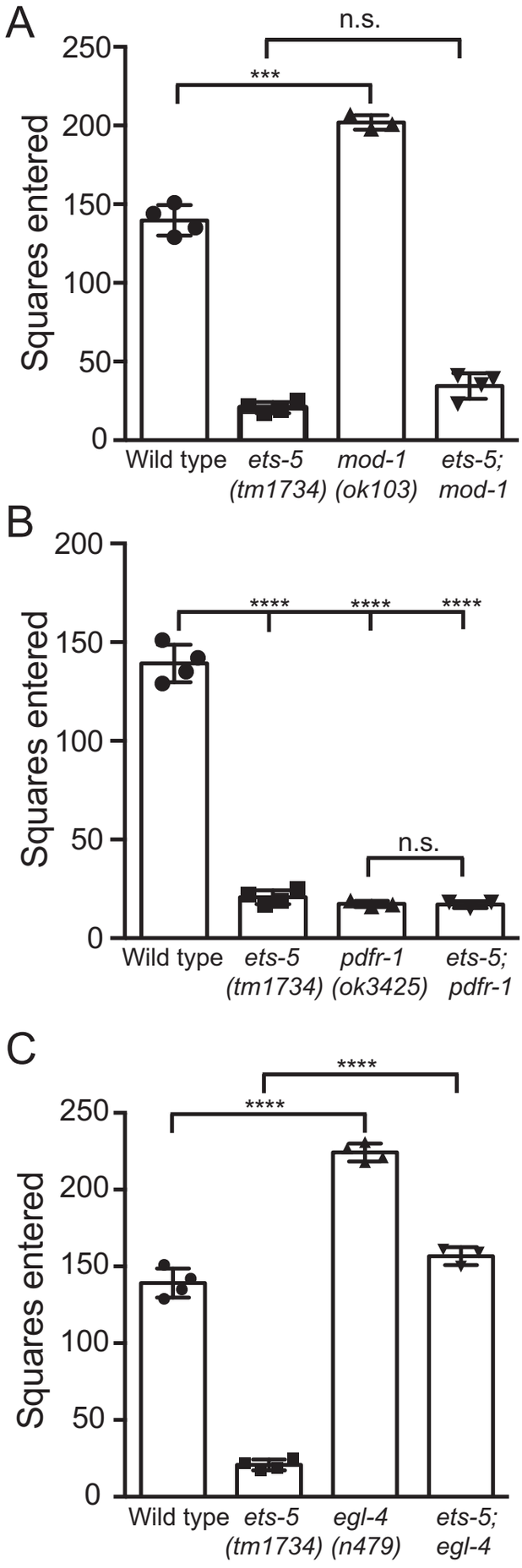

Fig. S3. Genetic epistasis analysis of *ets-5* exploration (related to Fig. 3). (*A*) Loss of *mod-1* leads to increased exploratory behavior. The *ets-5; mod-1* double mutant exhibits the *ets-5* single-mutant phenotype, suggesting that *ets-5* is epistatic to 5-HT signaling for exploratory behavior. ***$P < 0.001$ compared with WT; n.s., not significantly different compared with *ets-5(tm1734)*, ANOVA with Tukey's multiple comparisons test. (*B*) Loss of *pdfr-1* reduces exploratory behavior. The *ets-5; pdfr-1* double-mutant phenotype is no different from either single mutant. ****$P < 0.0001$ compared with WT; n.s., not significantly different compared with *pdfr-1(ok3425)*, ANOVA with Tukey's multiple comparisons test. (*C*) Loss of *egl-4* leads to increased exploratory behavior. The *ets-5; egl-4* double mutant exhibits WT levels of exploratory behavior, indicating that *egl-4*–regulated cGMP signaling is epistatic to *ets-5*. ****$P < 0.0001$ compared with WT or *ets-5(tm1734)*, ANOVA with Tukey's multiple comparisons test. We performed behavioral state analysis to further investigate the genetic relationship between these genes (Fig. 3).

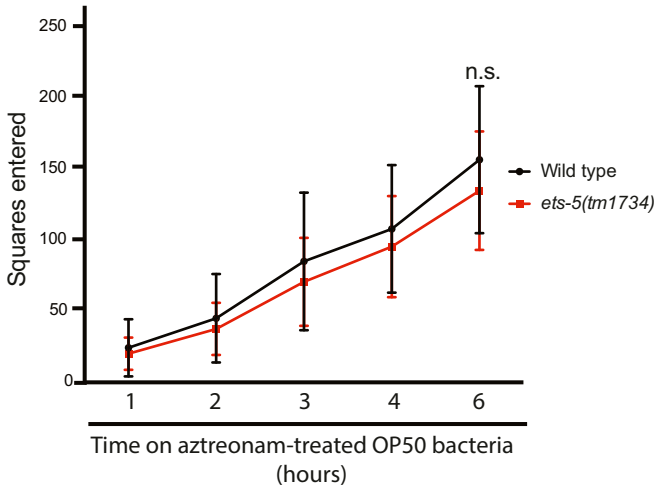

Fig. S4. *ets-5* mutant animals rapidly respond to starvation signals (related to Fig. 4). *ets-5(tm1734)* mutant animals behave similarly to WT when assayed on aztreonam-treated OP50 *E. coli* over a 6-h time course. Each time point shows the arithmetic means among repeats, with the error bar indicating SD. $n = 30$. n.s., not significantly different ($P > 0.05$), two-way ANOVA.

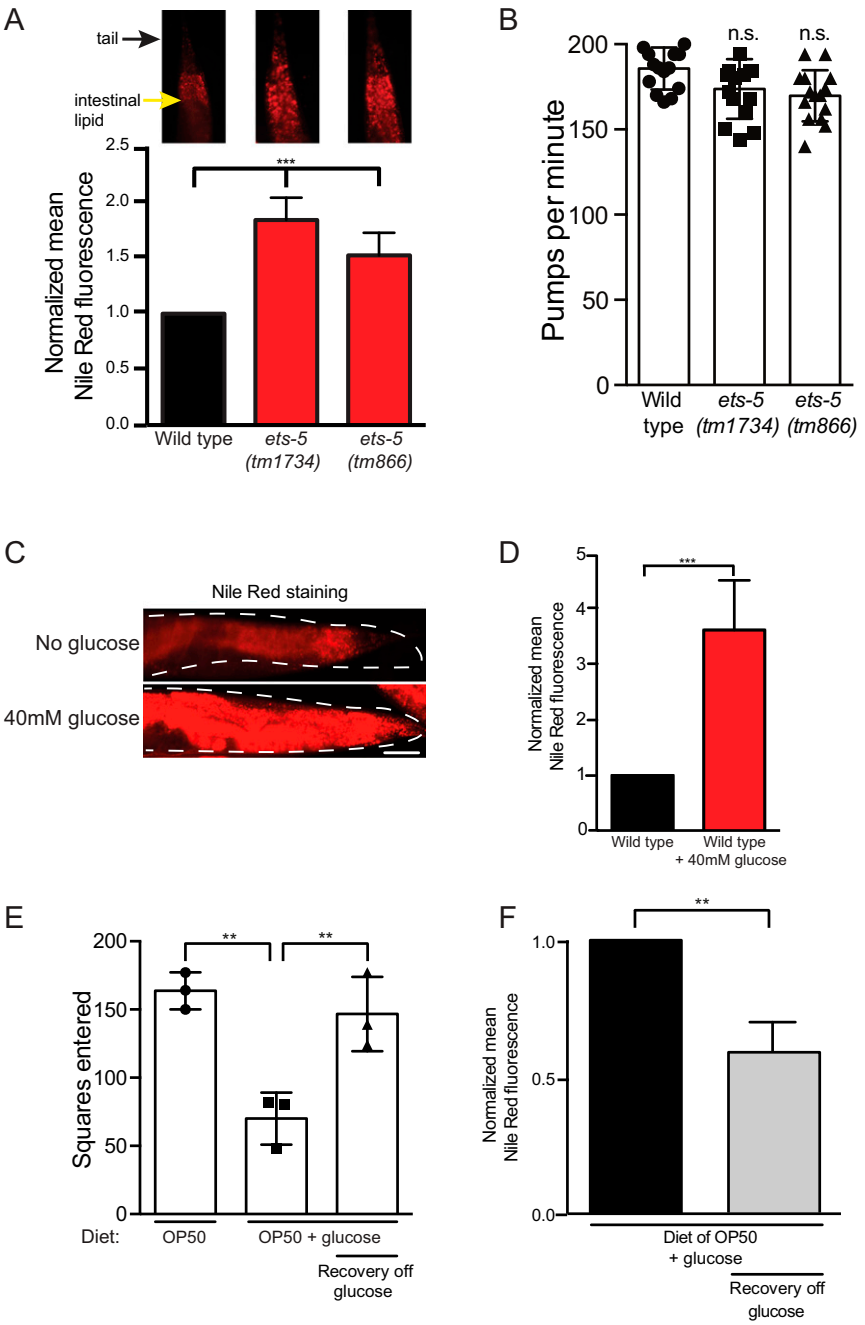

Fig. S5. Fat and feeding studies of WT and *ets-5(tm1734)* mutant animals (related to Fig. 5). (*A, Top*) Representative images of WT and *ets-5* mutant animals fixed and stained with Nile Red. Fat deposition in intestinal cells is visible as stained lipid droplets (yellow arrow). Animals are oriented facing downward with the tail (black arrow) at the posterior end. (*A, Bottom*) Quantification of Nile Red fluorescence in WT and *ets-5* mutant animals. $n = 30$. ***$P < 0.001$, unpaired *t* test. (*B*) The pumping rate of 1-d-old adult WT and *ets-5* mutant animals on an *E. coli* bacterial lawn. $n = 15$. n.s., not significantly different from WT animals, ANOVA with Tukey's multiple comparisons test. (*C*) Representative images of WT animals without glucose supplemented diet (*Top*) and with a high glucose diet (*Bottom*) fixed and stained with Nile Red. The tail region is shown, with posterior to the right. Worm outlined with dashes. (Scale bar: 20 μm.) (*D*) Quantification of fat content of WT animals cultivated with and without glucose supplementation. The no-glucose control was arbitrarily set to 1. ***$P <$ 0.0001, *t* test. (*E*) A high-glucose diet reduces exploratory behavior of WT animals, and recovery off glucose for 16 h restores WT exploratory behavior. $n >30$. **$P < 0.001$, ANOVA with Tukey's multiple comparisons test. (*F*) Quantification of Nile Red fluorescence of WT animals. Recovery from a high-glucose diet for 16 h reduces the level of fat stores. $n >30$. **$P < 0.01$, unpaired *t* test.